Experimental and computational evidence of solid-state anion–π and π–π interactions in $[VO(O_2)(L)(pa)]\cdot xH_2O$ complexes (L = picolinate, pyrazinate or quinolinate; pa = picolinamide)†

Róbert Gyepes,[a] Silvia Pacigová,[b] Michal Sivák*[b] and Jozef Tatiersky[b]

Received (in Montpellier, France) 12th November 2008, Accepted 11th February 2009
First published as an Advance Article on the web 23rd March 2009
DOI: 10.1039/b819875f

Two new neutral monoperoxidovanadium(V) complexes $[VO(O_2)(L)(pa)]\cdot xH_2O$ have been synthesized: $[VO(O_2)(pic)(pa)]\cdot H_2O$ (**1**) and $[VO(O_2)(Hquin)(pa)]\cdot 2H_2O$ (**2**) [pic: pyridine-2-carboxylato(1–) or picolinato(1–), Hquin: pyridine-2,3-dicarboxylato(1–) or quinolinato(1–), and pa: picolinamide]. The solid state structures of **1** and **2** feature a typical distorted pentagonal bipyramid coordination polyhedron around the central vanadium atoms. The bidentate anionic ligands are coordinated in two equatorial positions, while the bidentate picolinamide molecule is bound *via* the aromatic nitrogen and the carboxamide oxygen in one equatorial and one apical position. The experimental geometric parameters were used for a detailed study of intermolecular interactions between the pic–pic and pa–pa aromatic rings in **1**. Interestingly, no π–π interactions were observed between the pyridine rings of Hquin or pa in **2**, however, the less common anion–π solid-state interactions were found between the pic ligands in **1** and pca [pca = pyrazinecarboxylato(1–)] ligands in the already published structure of the related complex $[VO(O_2)(pca)(pa)]\cdot H_2O$ (**3**). The presence of anion–π and π–π interactions in **1** and **3** was confirmed by DFT computations performed on their solid-state structures. Computational results suggested a direct analogy between anion–π and π–π interactions, both being of predominantly electrostatic character.

Introduction

Due to the well known biological activity of pyridine- and pyrazinecarboxylic acids and their amides, both employed with success in pharmacology and medicine, together with the potential use of vanadium (IV/V) compounds in human and/or veterinarian medicine as insulin mimetics, it is of interest to study the products of mutual interaction between vanadium and the above mentioned organic substances, both in or without the presence of hydrogen peroxide. We have synthesized and structurally characterized more than 30 of the 72 currently known monoperoxidovanadium(V) complexes, with aminopolycarboxylates,[1] α-hydroxycarboxylates[2] or two different anionic or neutral organic ON or OO donor ligands.[3,4,5] The structural characterization of the latter type of complexes led us to formulate some empirical stereochemical rules for the occupation of the donor sites in the pentagonal bipyramid around the vanadium atom, depending on the chemical nature and charge of the coordinated ligands.[4,5]

Although the practice adopted in many papers dealing with structural studies is to confine the discussion of structure analysis only to the detailed description of the solid-state molecular structure(s), we have also paid some additional attention to the solid-state packing by analysing the intermolecular interactions and supramolecular architecture of the complexes of interest. As we have recently shown, the latter can be constructed for some complexes by the exclusive formation of π–π interactions and/or "non-classical" C–H···O hydrogen bonds between neighbouring molecules.[4]

The first theoretical investigation of anion–π interactions appeared in 1997.[6] Since 2002, when more ground-breaking papers devoted to theoretical investigations were published,[7] an increased attention has been paid to these interactions occurring in organic compounds, biomolecules and in coordination compounds as well. Papers dealing with this subject report either: i) theoretical calculations (*in vacuo*), ii) combined computational and crystallographic studies[8] or iii) investigations based on analysing the structural data from the Cambridge Structural Database.[9]

Anions involved in the reported anion–π interactions range from halogenides,[10] H^- or OH^-, through trigonal (NO_3^-,[11,12] CO_3^{2-},[13]) or tetrahedral (SO_4^{2-},[14] ClO_4^- [12,15]) oxidoanions, to halogenido anions[16] such as BF_4^- or PF_6^-, while the aromatic rings range from C_6F_6 through $C_6H_3F_3$[17] to five- or six-membered heterocycles containing one to three nitrogen atoms,[18] mostly triazine[19] and its derivatives. The investigations of group iii) are perfectly described in the recent paper.[9] However, for the particular case of vanadium

---

[a] *Department of Inorganic Chemistry, Charles University, Faculty of Natural Sciences, Albertov, 128 00 Prague, Czech Republic. E-mail: gyepes@natur.cuni.cz*
[b] *Department of Inorganic Chemistry, Comenius University, Faculty of Natural Sciences, Mlynská dolina, 842 15 Bratislava, Slovak Republic. E-mail: sivak@fns.uniba.sk; Fax: +421-2-60296273*

† CCDC reference numbers 705913 (for **1**) and 705914 (for **2**). For crystallographic data in CIF or other electronic format see DOI: 10.1039/b819875f

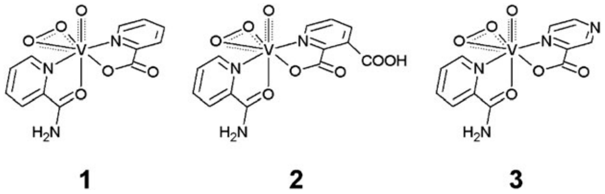

Scheme 1

chemistry, anion–π interactions between coordinated pca ligands were addressed for the first time as late as 2005 in our paper devoted to the structural characterization of the monoperoxido complex: $[NH_3(CH_2)_2NH_3][VO(O_2)(ox)(pca)]$.[20]

We present here, based both on single-crystal X-ray structural data† and DFT results for **1** and **3**, clear evidence that the solid-state structure, besides the expected π–π interactions, is stabilized further by intermolecular anion–π interactions between the negatively charged COO^- groups of the pic or pca ligands and their pyrazine or pyridine rings in two stacked complex molecules. The structural formulae of the neutral complexes **1–3** discussed in this paper are presented in Scheme 1.

Results and discussion

Experimental molecular structures and intermolecular interactions in 1 and 2

The molecular structure of **1** is shown in Fig. 1. The vanadium atom is displaced from the pentagonal plane (O2, O3, N12, O8, N2) of the distorted pentagonal bipyramid towards the O1 oxido ligand by 0.2643(4) Å (0.2402(6) Å for **3**, 0.254(2) and 0.274(2) Å for $[VO(O_2)(pic)(pcaa)(H_2O)]\cdot H_2O$ (**4**), pcaa = pyrazinamide[4]). The $V(\eta^2–O_2)$ group is asymmetric: the distance between the vanadium atom and O3 peroxido oxygen, which is involved in formation of more hydrogen bonds than O2 (Table 1), is markedly elongated. The supramolecular structure of **1** is built up incorporating several types of intermolecular interactions:

(i) π–π interactions between picolinamide ligands: the pyridine rings of pa form pairs of parallel, displaced π–π stacked rings with centroid (Ct) distance 3.589 Å, displacement angle 21.13° (defined as the angle between the Ct–Ct vector and ring normal to one of the pyridine planes[21]) and with trans oriented uncoordinated carboxamide functionalities. The distance between the parallel ring planes is 3.463 Å. The stacked rings are arranged in two differently oriented parallel planes and form a serpentine-like arrangement of stacked pa ligands along the crystallographic *b* axis (Fig. 2). The least-squares planes through two differently oriented pyridine rings of the pa ligands contain an angle of 22.05°.

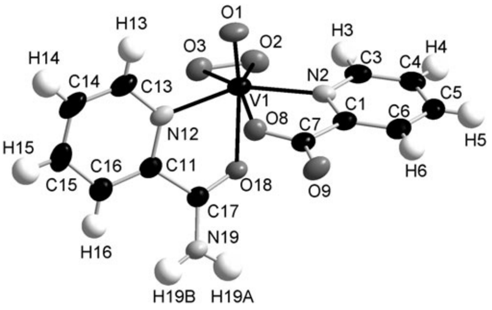

Fig. 1 Diamond presentation of the molecular structure of **1** with 50% probability ellipsoids. Selected interatomic distances (Å) and angles (°): V1–O1 1.5954(19), V1–O2 1.8774(15), V1–O3 1.8936(16), V1–O8 2.0311(14), V1–O18 2.2187(18), V1–N2 2.1265(21), V1–N12 2.1304(21), O2–O3 1.4162(28), O1–V1–O2 102.07(8), O1–V1–O3 100.78(8), O1–V1–O8 92.53(8), O1–V1–N2 98.93(9), O1–V1–N12 95.48(9), O1–V1–O18 166.31(8).

(ii) π–π and anion–π interactions between the picolinato ligands: even the pic ligands in **1** are arranged so that the pyridine rings lay in two differently oriented parallel planes, with the angle between the least-squares planes through two differently oriented pic ligands being 44.82°. The parallel planes are mutually arranged in an ABAB mode (Fig. 3). The AB planes are separated by 3.201 Å, but the ring centroid distance, CtA–CtB, is much longer (5.043 Å) than expected for π–π stacked rings. However, the mutual positions of the uncoordinated O9 oxygen atoms from the carboxylic groups (in the A plane) and the pyridine ring centroids CtB (and O9 in the B plane and CtA) is remarkable: the corresponding O9–CtB and O9–CtA distances are 3.272 Å, and the carboxylate O9 oxygen atoms are lying approximately on the ring normals (N2–CtB–O9 angle is 89.44°). These parameters, strongly suggestive of the existence of anion–π interactions, still rather rarely recognized in coordination compounds, were also a stimulus to supplement our studies with DFT calculations. In contrast to the AB planes, the separation distance between the BA planes (3.429 Å), displacement angle of 25.5° and the CtB–CtA distance (3.811 Å) for the parallelly displaced rings in the BA planes are typical values for π–π stacked rings.[21]These experimental data thus allowed us to assume the presence of simultaneous π–π and anion–π interactions between the parallel pic ligands in the structure of **1** (Fig. 3).

(iii) *hydrogen bonds*: the supramolecular structure is constructed also by *D*–H···O hydrogen bonds, where *D* = O, N or C (Table 1). Crystal water molecules form contacts with the peroxido oxygen atoms (O2, O3) and the uncoordinated O9 carboxylic oxygen atoms, which are concurrently involved in the anion–π interactions described above. The amide groups form hydrogen bonds with both peroxido oxygen atoms and the crystal water molecules. The network of hydrogen bonds is completed by a series of C–H···O bonds, fulfilling the criteria: H···O distance being smaller than 2.72 Å (sum of van der Waals radii) and the DHO angle being greater than 120°.

In the molecular structure of **2** (Fig. 4), the heptacoordinated vanadium atom is displaced by 0.2775(3) Å from the equatorial pentagonal plane of the bipyramid towards the triply bonded[4] oxido oxygen atom O31. The anion of the quinolinic acid, with a deprotonated carboxylic group in the 2 position, is coordinated as quinolinato(1–)-*N*,*O*[1] ligand, and pa, like in **1**, as a bidentate *N*[1],*O* ligand. All interatomic distances and bond angles within the coordination polyhedron are in the expected ranges. While atoms of the aromatic ring and those of the carboxamide group of pa lie almost in one plane, the planes of the protonated and uncoordinated carboxylic group and of the aromatic ring of Hquin are nearly

Table 1 D–H···O (D = O, N or C) hydrogen bonds distances (in Å) and D–H···A angles (in °) for **1** and **2** as calculated by PLATON

Hydrogen bond D–H···A	D–H	H···A	D···A	D–H···A	Sym. op. for A
For **1**					
N19–H19A···O2	0.93	2.23	3.066(3)	149	$x, \frac{1}{2}-y, -\frac{1}{2}+z$
N19–H19B···O20	0.94	1.92	2.862(3)	175	$1-x, \frac{1}{2}+y, \frac{1}{2}-z$
O20–H20A···O9	0.81(3)	2.01(3)	2.819(3)	172(4)	$1+x, y, z$
O20–H20B···O3	0.80(4)	2.04(4)	2.829(3)	168(4)	$x, \frac{1}{2}-y, -\frac{1}{2}+z$
C3–H3···O2	0.95	2.24	2.726(3)	111	
C4–H4···O3	0.95	2.46	3.104(3)	125	$1-x, \frac{1}{2}+y, \frac{3}{2}-z$
C4–H4···O18	0.95	2.53	3.133(3)	122	$1-x, -y, 1-z$
C13–H13···O9	0.95	2.39	3.261(3)	153	$x, \frac{1}{2}-y, \frac{1}{2}+z$
C15–H15···O8	0.95	2.41	3.134(3)	133	$-x, 1-y, 1-z$
C16–H16···O20	0.95	2.42	3.287(3)	152	$1-x, \frac{1}{2}+y, \frac{1}{2}-z$
For **2**					
O11–H11···O41	0.90(4)	1.69(3)	2.583(2)	170(4)	
N29–H29A···O12	0.87(2)	2.39(3)	2.910(2)	119(2)	$1+x, y, z$
N29–H29A···O33	0.87(2)	2.34(2)	3.148(2)	155(2)	$x, \frac{1}{2}-y, -\frac{1}{2}+z$
N29–H29B···O40	0.94(3)	1.89(3)	2.821(3)	177(3)	$1+x, y, z$
O40–H40A···O9	0.93(2)	1.93(3)	2.777	151(3)	
O40–H40B···O8	0.91(2)	1.96(2)	2.840(2)	164(3)	$1-x, 1-y, 1-z$
O41–H41A···O32	0.92(2)	2.49(2)	3.336(2)	153(2)	$-1+x, \frac{1}{2}-y, -\frac{1}{2}+z$
O41–H41A···O33	0.92(2)	1.89(2)	2.790(2)	165(2)	$-1+x, \frac{1}{2}-y, -\frac{1}{2}+z$
O41–H41B···O12	0.95	2.04(2)	2.962(2)	166(2)	$x, \frac{1}{2}-y, -\frac{1}{2}+z$
C23–H23···O40	0.95	2.30	3.223(3)	163	$1+x, y, z$
C25–H25···O32	0.95	2.43	3.069(2)	125	$2-x, \frac{1}{2}+y, \frac{3}{2}-z$

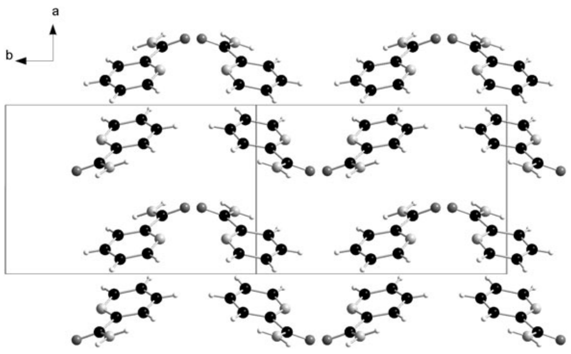

Fig. 2 Serpentine-like arrangement of the π–π stacked pa ligands in **1**, with two differently oriented parallel pyridine ring planes containing an angle of 22.05°.

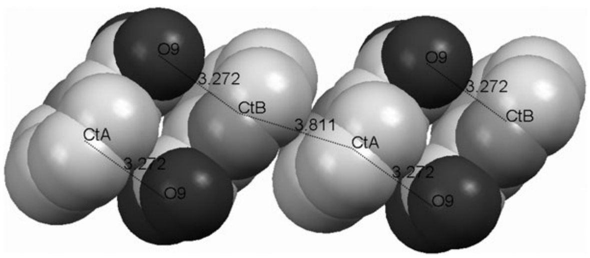

Fig. 3 Space-filling presentation of parallely arranged pic ligands in the structure of **1**. Viewing from left to right: with anion–π interactions between the carboxylic O9 oxygen atoms and rings with CtA and CtB centroids (3.272 Å), and π–π interactions between the rings with CtB and CtA centroids (3.811 Å).

perpendicular (89.18°). The pyridine rings of pa are arranged parallely, forming pairs, but the centroid distance between these pairs is too large (4.916 Å) to consider any significant π–π stacking between the rings. In addition, even the parameters for any two quin ligands in neighbouring complex molecules disallow the consideration of π–π or anion–π interactions: the observed ring centroid distances are 4.734 Å or 7.103 Å, and the ring centroid–uncoordinated carboxylic O9 oxygen atom distances are 5.993 Å and 5.796 Å. The structural data thus indicate that the supramolecular structure of **2** is built up exclusively from D–H···O (D = O, N or C) hydrogen bonds (Table 1). The shortest O···O distance (2.582 Å) was found between the protonated COOH group of Hquin and the oxygen atom of water molecule.

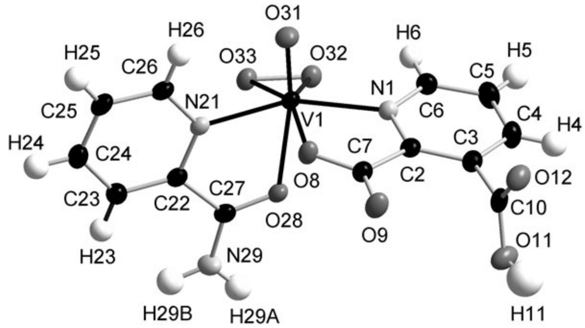

Fig. 4 Diamond presentation of the molecular structure of **2** with 50% probability ellipsoids. Selected interatomic distances (Å) and angles (°): V1–O31 1.5920(14), V1–O32 1.8647(13), V1–O33 1.9221(13), V1–O8 2.0466(13), V1–N21 2.1280(16), V1–N1 2.1490(15), V1–O28 2.1935(13), O32–O33 1.4242(18), O31–V1–O32 103.41(7), O31–V1–O33 100.47(6), O31–V1–O8 95.35(6), O31–V1–N21 93.84(7), O31–V1–N1 97.68(7), O31–V1–O28 166.71(6).

The two ON donor heteroligands in **1** and **2** coordinate in three equatorial and one apical positions of the bipyramid in complete accordance with the stereochemical rules we have empirically postulated for monoperoxidovanadium(v) complexes in our previous papers:[4,5]

(i) the nitrogen atoms, N2 and N12 (for **1**) and N1 and N21 (for **2**), occupy the cis positions with respect to the peroxido oxygen atoms, while the oxygen atoms, O8 and O18 the trans positions to the peroxido and oxido ligands, and

(ii) the anionic pic and Hquin ligands coordinate in two equatorial, and the neutral pa ligand in one equatorial and one apical positions.

The validity of these empirical rules has now been confirmed by X-ray single crystal structures of fifteen cationic, neutral or anionic $[VO(O_2)(L^1)(L^2)]$ complexes, where L^1 and L^2 are: ox-bpy, ox-phen,[5] ox-pic, ox-pca,[20] pic-bpy,[22] pic-phen,[23] pca-bpy, pca-phen,[4] pca-pa, pa-pa,[3] pic-pic,[22] pca-pca,[24] 3-OHpic-3OHpic,[25] and pic-pa (**1**), Hquin-pa (**2**).

Intermolecular π–π and anion–π interactions in $[VO(O_2)(pca)(pa)]\cdot H_2O$ (3)

The preparation and structural characterization of complex **3** was reported in our previous paper[3] without providing a detailed analysis of its solid-state intermolecular π–π interactions between the aromatic rings of pca and pa ligands. For complex **3**, we have overlooked (a frequent and usual phenomenon as recently analyzed and described[9]) in our original investigations[3] the intermolecular anion–π stabilization occurring between the neighbouring pca ligands. Since it has been noticed only after publishing, we address this issue in the present paper.

Similarly as in **1**, displaced π–π interactions between the pairs of pyridine rings of pa arranged in parallel AB planes occur in complex **3**: the centroid distance is 4.034 Å and the plane separation distance is 3.716 Å. The displacement angle is 22.5°. The carboxamide functionalities of the stacked rings are *anti* oriented. (Fig. 5). Unlike in the structure of **1** which has two different orientations of parallel planes of stacked rings of pa, these ligands are in **3** all arranged in parallel planes (Fig. 5).

Between the pyrazine rings and carboxylic groups of two pca ligands which are parallelly arranged in two planes (AB), the anion–π interactions are obviously predominant (Fig. 6). The distance between the ring centroid in plane B, Ct(B), and the uncoordinated carboxylic O5 oxygen atom[3] originating from the pca located in plane A is 3.328 Å. The separation distance between the AB planes is 3.268 Å. The large Ct(A)–Ct(B) centroid distance 4.573 Å indicates that besides the anion–π interactions some additional (albeit slight) attractive π–π stacking between the pyrazine rings is still present.

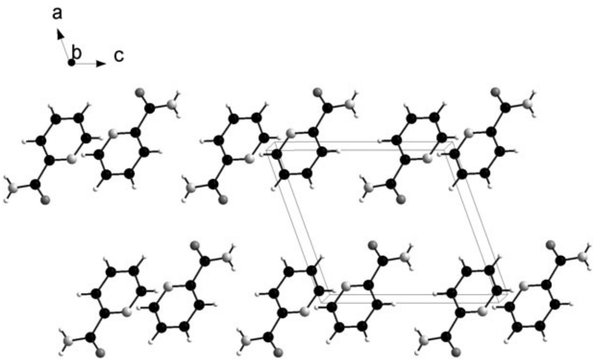

Fig. 5 The parallel displaced pairs of π–π stacked pa ligands in **3** with *anti* oriented carboxamide functionalities. Centroid and plane separation distances are 4.034 Å and 3.716 Å, respectively.

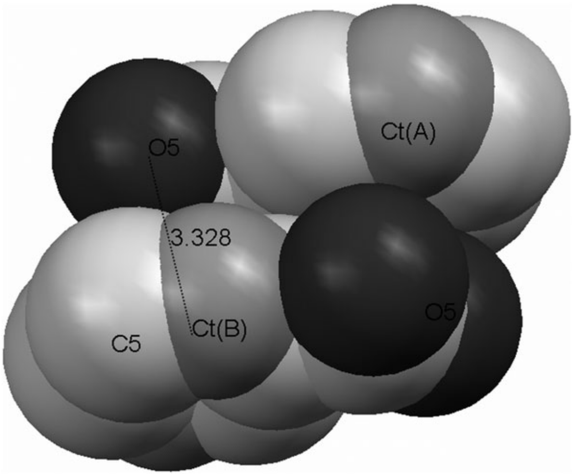

Fig. 6 Space-filling presentation of a pair of pca ligands in the structure of **3**, stacked due to anion–π interactions between the uncoordinated O5 oxygen atoms of the COO^- groups and pyrazine rings.

Table 2 The coordination modes of the heteroligands and types of intermolecular π–π interactions observed for **1–4**

Complex	Coordination modes	Intermolecular π interactions
$[VO(O_2)(pic)(pa)]\cdot H_2O$ (**1**)	pic(1−)-*N*,*O*	parallel displaced π–π + anion–π
	pa-*N*^{1},*O*	parallel displaced π–π
$[VO(O_2)(Hquin)(pa)]\cdot 2H_2O$ (**2**)	Hquin(1−)-*N*,*O*	none
	pa-*N*^{1},*O*	none
$[VO(O_2)(pca)(pa)]\cdot H_2O$ (**3**)	pca(1−)-*N*^{1},*O*	anion–π + weak π–π
	pa-*N*,*O*	parallel displaced π–π
$[VO(O_2)(pic)(pcaa)(H_2O)]\cdot H_2O$ (**4**)	pic(1−)-*N*,*O*	non-parallel π–π
	pcaa-*N*^{4}	none

To confirm the existence of the discussed anion–π interactions in **3**, we have also performed DFT calculations for this complex (*vide infra*).

Despite the fact that the chemical composition of complexes **1–3**, and of even the earlier characterized complex **4**,[4] is very similar (they differ only in the anionic heteroligands: pic, Hquin, pca or in the amides: pa, pcaa), the complexes **1–4** exhibit, apart from hydrogen bonding networks, some substantial differences in the types of intermolecular π–π interactions contributing to the stabilization of their supramolecular structures (Table 2). There is an especially significant difference in the nature of the intermolecular interactions in complexes **1** and **2**, although they differ in the chemical composition of the complex molecules by just one COOH group in **2**. In the latter complex, no π–π stacking was found.

The complexes **1** and **2** crystallize as racemic compounds (crystalline racemates, in which the two enantiomers are present in equal amounts in a well defined arrangement within the lattice[26]).

DFT calculations

For a theoretical insight into the nature of anion–π interactions, identified based on experimental structural data, we have performed DFT calculations for the solid-state structures of both **1** and **3**, since to our best knowledge, these are the first calculations for solid-state structures in which anion–π interactions between two coordinated aromatic carboxylates exist.

Theoretical studies dealing with solid-state interactions require the application of Bloch wavefunctions, since the periodic modulation generated by the crystal lattice should be also accounted for in the wavefunction of the system under study. The requirement for Bloch wavefunctions for our systems was clearly evidenced by a preliminary study performed on two adjacent molecules forming a stacked pair in **3**, aimed at reproducing the energy minimum between two neighbouring molecules oriented exactly as in the experimental solid-state structure. The expected energy minimum however could not be achieved when periodic boundary conditions were neglected—the total energy of this model system showed an exponential decrease with the increasing separation of the two molecules. This result clearly indicated that the inclusion of an external periodic potential was of vital importance for any further studies of solid-state arrangements, since omitting the periodic replication could lead to false conclusions. Subsequent DFT calculations of **1** and **3** were thus conducted on whole unit cells obtained from X-ray single crystal analyses and with periodic boundary conditions properly included. Due to the demanding nature of such computations, however, no geometry optimizations could be attempted and all calculations were carried out as single-point only.

The most significant contribution to the π–π stabilization of aromatic molecules was already suggested by Hunter and Sanders[27] to be of an electrostatic nature, presumably as the result of balancing the π–σ attractive and π–π repulsive electrostatic interactions of the adjacent aromatic rings. The contribution from van der Waals interactions, though always attractive at interplanar separations between aromatic rings occurring in solid-state structures, was found to be of minor importance only.[28]

Furthermore, covalent interactions cannot be a driving force in stabilizing solid-state structures. Although π systems on adjacent molecules may generate some mutual overlap, any possible attractive overlaps are inherently counterbalanced by the corresponding repulsive interaction between the same partners, generating a net overall repulsion. This phenomenon is illustrated in Fig. 7, depicting the simultaneous attraction (orb. 153) and repulsion (orb. 162) between one set of π orbitals between two adjacent pca ligands. (The repulsion is of maximum magnitude with a face-to-face arrangement between two aromatic rings, since such an arrangement will bring the same π orbitals of both partners into proximity allowing for the best mutual overlap.)

These results demonstrate that although occurring between covalent aromatic systems, discussions of π–π interactions can be safely confined to the analysis of distribution of the electrostatic potential over the aromatic rings.

Although anion–π interactions represent a somewhat different approach to the model of interacting charges, they are similar to π–π interactions in their genesis. In contrast to the case of π–π stacking, which usually takes place between groups consisting of several atoms, the anionic partner in the anion–π stabilization is only a single atom (carboxylate oxygen) in our case. Contrary to aromatic rings, which represent a system of alternating positive/negative regions of electrostatic potential, the distribution of the electrostatic potential on anions is of much higher uniformity. This fact suggests that in seeking for intramolecular stabilization, anions will strongly prefer the most positive regions of their partners; for the particular case of aromatic rings this region is practically coincident with the ring centroid.

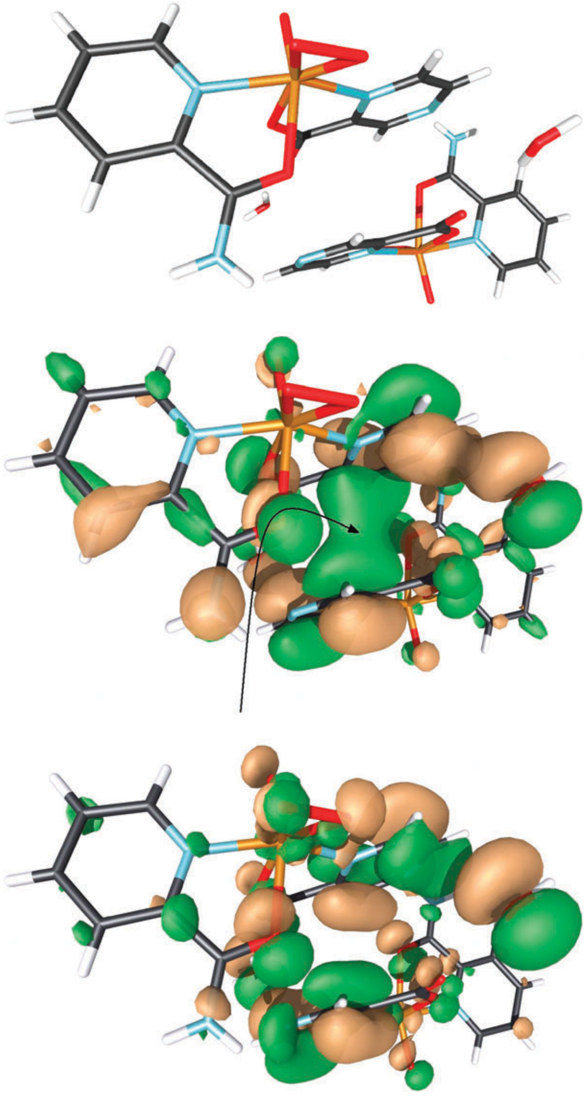

Fig. 7 Perspective view of two adjacent molecules of **3** (top) and canonical orbitals 153 (centre, 2%) and 162 (bottom; 2%) of **3** depicting the attractive (see arrow) and corresponding repulsive covalent interactions between two adjacent pca ligands. Both orbitals are doubly occupied.

Based on these assumptions, the solid-state packing of both **1** and **3** can be understood. Complex **3** features a remarkable anion–π interaction between a pair of neighbouring pca ligands with one carboxylato oxygen located above the centroid of the adjacent pca skeleton (Fig. 8). Not only is the overall electron density of the aromatic ring lowest in the ring centre, but the electrostatic potential is also positive,

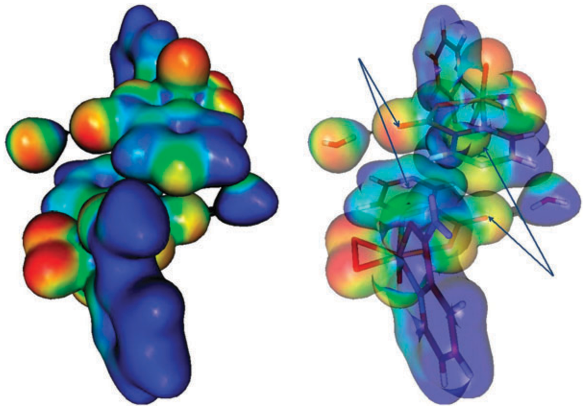

Fig. 8 Isodensity surface (2%) colour-coded by electrostatic potential for two adjacent molecules of **3**, depicting the anion–π interaction. Colour legend for the electrostatic potential: red < -0.1; yellow $= -0.05$; green $= 0.00$; light blue $= 0.05$; deep blue > 0.1). The picture on the right visualizes the orientation of individual atoms in the electron density cloud; the arrows mark the two anion–π interacting centres (pca ligands).

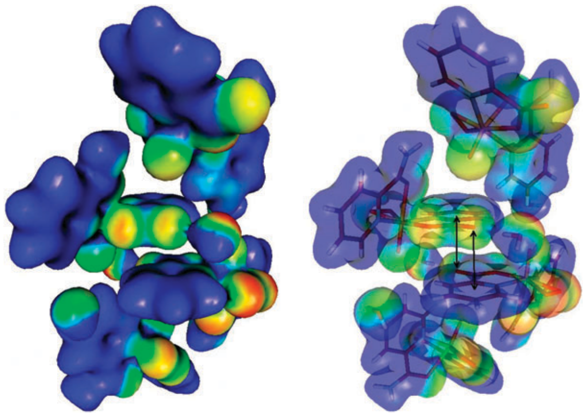

Fig. 9 Isodensity surface (2%) colour- coded by electrostatic potential for the unit cell of **1**. The two molecules in the unit cell were transformed for an easier visualization of their interaction. Colour legend for the electrostatic potential: red < -0.1; yellow $= -0.05$; green $= 0.00$; light blue $= 0.05$; deep blue > 0.1. The picture on the right visualizes the orientation of individual atoms in the electron density cloud; the arrows mark the two anion–π interacting pic ligands.

providing a preferential position for a negatively charged partner.

Complex **1** is very similar in its solid-state architecture: the dominating anion–π interactions occur between a pair of neighbouring pic ligands (Fig. 9). The requirement for a negatively charged partner, preferably approaching only the centre of the aromatic ring, explains many geometrical aspects of **1** and **3**, since both structures possess several oxygen anions for potential intermolecular electrostatic interactions. As with the case of π–π interactions where a face-to-face arrangement results in a net repulsion, anionic groups approaching the σ skeleton of the six-member rings are also disallowed. The best stabilizing effect is thus achieved with single atoms having smaller ionic radii.

Conclusions

The analysis of structural data obtained for two new monoperoxidovanadium(V) complexes, $[VO(O_2)(pic)(pa)]\cdot H_2O$ (**1**) and $[VO(O_2)(Hquin)(pa)]\cdot 2H_2O$ (**2**), and for the recently characterized $[VO(O_2)(pca)(pa)]\cdot H_2O$ (**3**),[3] allowed us to also recognize, besides D–H···O (D = O, N or C) hydrogen bonds (in **1–3**) and π–π stacking (in **1** and **3**), intermolecular anion–π interactions (in **1** and **3**) between coordinated pic or pca anions of two complex molecules as important contacts contributing to structure stabilization. The latter interactions were confirmed by DFT calculations on the solid-state structures of **1** and **3**, and shown to be mostly of electrostatic character. The structures of **1** and **3**, enlarging the group of structurally characterized bis(ON-heteroligand) monoperoxidovandium(V) complexes now to fifteen, have again verified the validity of our empirical stereochemical rules for occupation of the four donor sites in pentagonal bipyramidal mononuclear monoperoxidovanadium complexes formulated earlier.[4,5]

Experimental

Chemicals and methods

V_2O_5 was prepared by thermal decomposition of previously purified NH_4VO_3. Other chemicals (analytical grade) were used as supplied by Aldrich, Lachema or Slavus. The IR spectra in nujol mulls were registered on a FT IR Nicolet Magna 750 spectrometer (400–1800 cm^{-1}). The ^{51}V NMR spectra were registered at 278 K on a Varian Mercury Plus spectrometer (B_0 = 7.05 T, 78.9 MHz operating frequency) at concentration of complexes 0.01 mol/dm^3. The δ_V values are related to $VOCl_3$ as external standard. C, H, and N were determined on a 1106 CHN-analyzer (Carlo Erba). Vanadium was determined in samples previously annealed to V_2O_5 and then dissolved in a KOH solution by titration with $FeSO_4$ (c = 0.1 mol/dm^3) and diphenylamine as indicator.

Syntheses

$[VO(O_2)(pic)(pa)]\cdot H_2O$, (1). *Solution A*: V_2O_5 (0.181 g, 1.00 mmol) was dissolved in H_2O_2 (3.0 cm^3, 30%) under cooling in ice bath. *Solution B*: picolinamide (0.244 g, 2.00 mmol) was dissolved in 5.0 cm^3 water. It was then added dropwise to the solution *A*. The pH of the resulting red solution was 1.7. To this solution, a cooled solution of picolinic acid (0.246 g, 2.00 mmol), prepared by dissolution in 10.0 cm^3 water (pH = 3), was slowly added (resulting pH 1.85). To the final reaction solution, isopropylalcohol (15.0 cm^3) was added to initialize the crystallization. The red crystalline product was formed within 2–3 days, and it was isolated and dried above silica gel and stored at 7 °C in refrigerator. The complex is almost insoluble in water, MeOH, EtOH, *i*-PrOH, PrOH, acetonitrile, but dissolves well in dimethylformamide (DMF). Found: C, 39.4; H, 2.3; N, 10.9; V, 13.3. $C_{12}H_{12}N_3O_7V$ requires C, 40.0; H, 3.35; N, 11.6; V, 14.1%. $\tilde{\nu}$/cm^{-1}: 414 w, 424 m, 444 m, 455 m, 532 m, 547 m and 575 m [ν(V–O$_p$)], 654 s, 688 m, 711 s, 721 m, 764 s, 771 s sh, 828 m, 860 s, 907 s, 940 vs [ν(O$_p$–O$_p$)], 968 vs [ν(V$\equiv$O], 1012 w, 1031 s, 1055 s, 1091 m, 1118 m, 1157 w, 1178 m, 1237 m, 1265 m, 1299 s, 1363 vs, 1380 vs $[\nu_s(COO)]$, 1456 sh s, 1463 vs, 1571 vs, 1607 vs and 1660 vs $[\nu_s(COO) + \delta(H_2O)]$, 1689vs. $[\nu(C{=}O)]$. δ_V/I_{rel} (in DMF), ppm/%: −530.34/63.3, −556.52/36.7.

[VO(O$_2$)(Hquin)(pa)]·2H$_2$O, (2). *Solution A:* V_2O_5 (0.181 g, 1.00 mmol) was dissolved in H_2O_2 (3.0 cm^3, 30%) under cooling in ice bath. *Solution B:* picolinamide (0.244 g, 2.00 mmol) was dissolved in 30.0 cm^3 water and added dropwise to the solution *A* (resulting pH was 1.9). Afterwards, quinolinic acid (0.334 g, 2.00 mmol) was dissolved in 15.0 cm^3 of hot water (pH 3) and slowly added to the solution *A* + *B*. The final pH of the resulting dark red solution was 1.8. To initialize the crystallization, 15.0 cm^3 of isopropylalcohol were added. A red crystalline product was formed within 3–5 days, and it was isolated, dried and stored as for **1**. The complex is less soluble in water and MeOH, insoluble in EtOH, PrOH and *i*-PrOH, but dissolves well in acetone, acetonitrile and DMF. Found: C, 36.4; H, 3.2; N, 9.8; V, 12.15. $C_{13}H_{14}N_3O_{10}V$ requires C, 36.9; H, 3.3; N, 9.9; V, 12.0%. $\tilde{\nu}$/cm^{-1}: 421 m, 432 w, 454 m, 469 m, 512 s, 556 m $[\nu(V–O_p)]$, 592 m, 610 w, 653 m, 660 m, 684 s, 697 vs, 772 m, 790 w, 821 s, 832 sh, 873 m, 911 w, 941 vs $[\nu(O_p–O_p)]$, 974 vs $[\nu(V{\equiv}O]$, 1000 w, 1031 m, 1059 w, 1107 s, 1127 m, 1150 m, 1161 w, 1173 w, 1225 m, 1271 s, 1311 s, 1350 vs, 1377 s $[\nu_s(COO)]$, 1453 s, 1462 vs, 1498 m, 1571 vs, 1590 vs, 1623 s and 1674 vs $[\nu_{as}(COO) + \delta(H_2O)]$, 1692 vs $[\nu(C{=}O)]$, 1706 sh vs $[\nu(COOH)]$, 1781 vw. δ_V/I_{rel} (in H_2O), ppm/%: −585.07/8.1, −604.1/69.0, −626.32/22.9; the complex decomposes on dissolution to species with chemical shifts assignable to the following complexes (with published chemical shifts in parenthesis): $[VO(O_2)(pa)(H_2O)_x]^+$ (−587),[3] $[VO(O_2)(pa)_2]^+$ (−603)[3] and $[VO(O_2)(quin)_2]^{n-}$ (−628.9);[29] δ_V/I_{rel} (in DMF), ppm/%: −525.59/66.3, −549.38/32.2.

X-ray single-crystal analysis

Single crystals of **1** and **2** were mounted onto glass rods. Diffraction data were collected at 150 K on a Nonius KappaCCD diffractometer (MoKα radiation, λ = 0.71073 Å) and processed by the HKL program package.[30] The phase problem was solved by direct methods (SIR97),[31] and refined by full matrix least squares on F^2 (SHELXL-97).[32] All non hydrogen atoms were refined anisotropically. Any hydrogen atoms attached to oxygen or nitrogen atoms were refined isotropically while all hydrogen atoms attached to carbon atoms were included in ideal positions and refined isotropically using the riding model. Due to the lower quality of data for **2**, the O–H distances on both crystal water molecules were restrained to 0.97(2) Å. The figures were prepared by Diamond.[33]

Crystal data for 1†. $C_{12}H_{12}N_3O_7V$, M_r = 361.19, monoclinic, space group $P2_1/c$ (no. 14), a = 8.6180(4) Å, b = 12.4218(8) Å, c = 13.6060(7) Å, β = 104.255(3)°, V = 1411.69(13) Å^3, Z = 4, T = 150.0(1) K, ρ_{calc} = 1.699 g/cm^3, μ = 0.746 mm^{-1}, 11336 reflections measured, 3244 unique (R_{int} = 3.7%). The final $wR(F^2)$ was 0.0959 (all data).

Crystal data for 2†. $C_{13}H_{14}N_3O_{10}V$, M_r = 423.21, monoclinic, space group $P2_1/c$ (no. 14), a = 9.6949(3), b = 14.4076(5), c = 11.6205(3) Å, β = 96.242(2)°, V = 1613.53(9) Å^3, Z = 4, T = 150.0(1) K, ρ_{calc} = 1.742 g/cm^3, μ = 0.680 mm^{-1}, 7084 reflections measured, 3711 unique (R_{int} = 3.6%). The final $wR(F^2)$ was 0.0946 (all data).

Computational details

DFT computations were conducted at the *fermi* cluster located at the Computer Centre of the J. Heyrovský Institute of Physical Chemistry, Academy of Sciences of the Czech Republic, using Gaussian 03, Revision E.01.[34] Calculations were performed on whole unit cells obtained from X-ray single-crystal structure studies. To make visualization easier, the unit cells obtained from diffraction experiments were transformed so that the molecules in the anion–π interaction were located within one unit cell. No atoms were neglected. To fit available computer resources, the number of unit cells was limited to 200 for both **1** and **3**. The LANL2DZ ECP was used for the vanadium atoms; for all remaining atoms the 6-31G(d) basis set was used for **3** and the 6-31G basis set for **1**. Geometry optimizations were not attempted. Analysis, visualization of individual molecular orbitals and the overall electrostatic potential was accomplished by Molden.[35]

Acknowledgements

This investigation has been supported by the Ministry of Education of the Slovak Republic (Grant VEGA 1/4462/07), Comenius University in Bratislava (young scientists' grant UK/277/2008), and the Ministry of Education of the Czech Republic (Grant MSM0021620857). NMR measurements were performed on the equipment supported by the Slovak State Programme Project No. 2003SP200280203.

References

1 A. E. Lapshin, Y. I. Smolin, Y. F. Shepelev, M. Sivák and D. Gyepesová, *Acta Crystallogr., Sect. C*, 1993, **49**, 867–870; A. E. Lapshin, Y. I. Smolin, Y. F. Shepelev, P. Schwendt and D. Gyepesová, *Kristallografiya*, 1992, **37**, 1415–1423; M. Sivák, J. Tyršelová, F. Pavelčík and J. Marek, *Polyhedron*, 1996, **15**, 1057–1062; L'. Kuchta, M. Sivák, J. Marek, F. Pavelčík and M. Časný, *New J. Chem.*, 1999, **23**, 43–46; M. Sivák, M. Mad'arová, J. Tatiersky and J. Marek, *Eur. J. Inorg. Chem.*, 2003, 2075–2081.

2 I. Kutá-Smatanová, J. Marek, P. Švančárek and P. Schwendt, *Acta Crystallogr., Sect. C*, 2000, **56**, 154–155; P. Schwendt, P. Švančárek, I. Smatanová and J. Marek, *J. Inorg. Biochem.*, 2000, **80**, 59–64; M. Ahmed, P. Schwendt, J. Marek and M. Sivák, *Polyhedron*, 2004, **23**, 655–663; M. Ahmed, P. Schwendt and M. Sivák, *Transition Met. Chem.*, 2004, **29**, 675–680; P. Schwendt, M. Ahmed and J. Marek, *Inorg. Chim. Acta*, 2005, **358**, 3572–3580.

3 M. Mad'arová, M. Sivák, L'. Kuchta, J. Marek and J. Benko, *Dalton Trans.*, 2004, 3313–3320.

4 S. Pacigová, R. Gyepes, J. Tatiersky and M. Sivák, *Dalton Trans.*, 2008, 121–130.

5 J. Tatiersky, P. Schwendt, J. Marek and M. Sivák, *New J. Chem.*, 2004, **28**, 127–133.

6 I. Alkorta, I. Rozas and J. Elguero, *J. Org. Chem.*, 1997, **62**, 4687–4691.

7 D. Quinonero, C. Garau, C. Rotger, A. Frontera, P. Ballester, A. Costa and P. M. Deya, *Angew. Chem., Int. Ed.*, 2002, **41**, 3389–3392; I. Alkorta, I. Rozas and J. Elguero, *J. Am. Chem. Soc.*, 2002, **124**, 8593–8598; M. Mascal, A. Armstrong and M. Bartberger, *J. Am. Chem. Soc.*, 2002, **124**, 6274–6276.

8 A. Frontera, F. Saczewski, M. Gdaniec, E. Dziemidowicz-Borys, A. Kurland, P. M. Deya, D. Quinonero and C. Garau, *Chem.–Eur. J.*, 2005, **11**, 6560–6567; T. J. Mooibroek, S. J. Teat, C. Massera, P. Gamez and J. Reedijk, *Cryst. Growth Des.*, 2006, **6**, 1569–1574.

9 T. J. Mooibroek, C. A. Black and J. Reedijk, *Cryst. Growth Des.*, 2008, **8**, 1082–1093.

10 C. Garau, D. Quinonero, A. Frontera, P. Ballester, A. Costa and P. M. Deya, *J. Phys. Chem. A*, 2005, **109**, 9341–9345; T. Dorn, C. Janiak and K. Abu-Shandi, *CrystEngComm*, 2005, **7**, 633–641; Y. S. Rosokha, S. V. Lindemann, S. V. Rosokha and J. K. Kochi, *Angew. Chem., Int. Ed.*, 2005, **44**, 2178–2178; P. de Hoog, P. Gamez, I. Mutikainen, U. Turpeinen and J. Reedijk, *Angew. Chem., Int. Ed.*, 2004, **43**, 5815–5817.

11 P. U. Mahaswari, B. Modec, A. Pevec, B. Kozlevcar, C. Massera, P. Gamez and J. Reedijk, *Inorg. Chem.*, 2006, **45**, 6637–6645.

12 C. A. Black, L. R. Hanton and M. D. Spicer, *Inorg. Chem.*, 2007, **46**, 3669–3679.

13 D. Kim, P. Tarakeshwar and K. S. Kim, *J. Phys. Chem. A*, 2004, **108**, 1250–1258.

14 K. V. Domasewitch, I. A. Gural'skij, P. V. Solntsev, E. B. Rusanov and A. N. Chernega, *Acta Crystallogr., Sect. C*, 2007, **63**, m259–m263.

15 L. A. Barrios, G. Aromi, A. Frontera, D. Quinonero, P. M. Deya, P. Gamez, O. Roubeau, E. J. Shotton and S. J. Teat, *Inorg. Chem.*, 2008, **47**, 5873–5881.

16 D. L. Reger, R. P. Watson and M. D. Smith, *Inorg. Chem.*, 2006, **45**, 10077–10087.

17 D. Quinonero, C. Garau, A. Frontera, P. Ballester, A. Costa and P. M. Deya, *J. Phys. Chem. A*, 2005, **109**, 4632–4637.

18 H. Casellas, G. Massera, P. Gamez, A. M. M. Lanfredi and J. Reedijk, *Eur. J. Inorg. Chem.*, 2005, **14**, 2902–2908.

19 T. J. Mooibroek and P. Gamez, *Inorg. Chim. Acta*, 2007, **360**, 381–404.

20 J. Tatiersky, P. Schwendt, M. Sivák and J. Marek, *Dalton Trans.*, 2005, 2305–2311.

21 Ch. Janiak, *J. Chem. Soc., Dalton Trans.*, 2000, 3885–3896.

22 H. Szentivanyi and R. Stomberg, *Acta Chem. Scand., Ser. A*, 1982, **37**, 709–714.

23 V. S. Sergienko, M. A. Porai-Koshits, V. K. Borzunov and A. B. Ilyukhin, *Russ. J. Coord. Chem.*, 1993, **19**, 714–728.

24 G. Süss-Fink, S. Stanislas, G. B. Shul̆pin, G. Nizova, H. Stoeckli-Evans, A. Neels, Ch. Bobillier and S. Claude, *J. Chem. Soc., Dalton Trans.*, 1999, 3169–3175.

25 M. Časný and D. Rehder, *Dalton Trans.*, 2004, 839–846.

26 G. P. Moss, (IUPAC Recommendations 1996), *Pure Appl. Chem.*, 1996, **68**, 2193–2222.

27 C. A. Hunter and J. K. M. Sanders, *J. Am. Chem. Soc.*, 1990, **112**, 5525–5534.

28 M. Rigby, E. B. Smith, W. A. Wakeham and G. C. Maitland, in *The Forces between Molecules*, Clarendon, Oxford, 1986; A. D. Buckingham, in *Intermolecular Interactions: From Diatomics to Biopolymers*, ed. B. Pullman, Wiley, Chichester, 1978, pp. 1–68; J. Caillet and P. Claverie, *Acta Crystallogr., Sect. A*, 1975, **31**, 448–461.

29 O. Vollárová, J. Benko and M. Sivák, *Collect. Czech. Chem. Commun.*, 1996, **61**, 574–588.

30 Z. Otwinowski and W. Minor, *HKL Denzo and Scalepack program package by Nonius*. For a reference see Z. Otwinowski and W. Minor, *Methods Enzymol.*, 1997, **276**, 307–326.

31 A. Altomare, M. C. Burla, M. Camalli, G. Cascarano, C. Giacovazzo, A. Guagliardi and G. J. Polidori, *Appl. Crystallogr., Sect. A*, 1994, **27**, 435–436.

32 G. M. Sheldrick, *SHELXL97. Program for Crystal Structure Refinement from Diffraction Data*, University of Göttingen, Göttingen, 1997.

33 DIAMOND, Version 3.1f, CRYSTAL IMPACT, Postfach 1251, 53002 Bonn, Germany. (URL: www.crystalimpact.com/diamond).

34 M. J. Frisch, G. W. Trucks, H. B. Schlegel, G. E. Scuseria, M. A. Robb, J. R. Cheeseman, J. A. Montgomery, Jr, T. Vreven, K. N. Kudin, J. C. Burant, J. M. Millam, S. S. Iyengar, J. Tomasi, V. Barone, B. Mennucci, M. Cossi, G. Scalmani, N. Rega, G. A. Petersson, H. Nakatsuji, M. Hada, M. Ehara, K. Toyota, R. Fukuda, J. Hasegawa, M. Ishida, T. Nakajima, Y. Honda, O. Kitao, H. Nakai, M. Klene, X. Li, J. E. Knox, H. P. Hratchian, J. B. Cross, V. Bakken, C. Adamo, J. Jaramillo, R. Gomperts, R. E. Stratmann, O. Yazyev, A. J. Austin, R. Cammi, C. Pomelli, J. W. Ochterski, P. Y. Ayala, K. Morokuma, G. A. Voth, P. Salvador, J. J. Dannenberg, V. G. Zakrzewski, S. Dapprich, A. D. Daniels, M. C. Strain, Ö. Farkas, D. K. Malick, A. D. Rabuck, K. Raghavachari, J. B. Foresman, J. V. Ortiz, Q. Cui, A. G. Baboul, S. Clifford, J. Cioslowski, B. B. Stefanov, G. Liu, A. Liashenko, P. Piskorz, I. Komaromi, R. L. Martin, D. J. Fox, T. Keith, M. A. Al-Laham, C. Y. Peng, A. Nanayakkara, M. Challacombe, P. M. W. Gill, B. Johnson, W. Chen, M. W. Wong, C. Gonzalez and J. A. Pople, *GAUSSIAN 03, Revision E.01*, Gaussian, Inc., Wallingford CT, 2004.

35 G. Schaftenaar and J. H. Noordik, *J. Comput.–Aided Mol. Des.*, 2000, **14**, 123–134.